

Full length article

Structural instabilities during cyclic loading of ultrafine-grained copper studied with micro bending experiments

M.W. Kapp^{a,*}, T. Kremmer^{a,b}, C. Motz^{a,c}, B. Yang^a, R. Pippan^a^a Erich Schmid Institute of Materials Science, Austrian Academy of Sciences, Jahnstr. 12, 8700, Leoben, Austria^b Chair of Nonferrous Metallurgy, University of Leoben, Franz-Josef-Str. 18, 8700, Leoben, Austria^c Department Materials Science and Engineering, Saarland University, Gebäude D2.2, 66041, Saarbrücken, Germany

ARTICLE INFO

Article history:

Received 22 August 2016

Received in revised form

8 November 2016

Accepted 17 November 2016

Available online 18 December 2016

Keywords:

Severe plastic deformation

Low cycle fatigue

Cyclic softening

Grain growth

Grain boundary migration

ABSTRACT

The cyclic mechanical properties and microstructural stability of severe plastically deformed copper were investigated by means of micro bending experiments. The ultrafine-grained structure of OFHC copper was synthesized utilizing the high pressure torsion (HPT) technique. Micron sized cantilevers were focused-ion-beam milled and subsequently tested within a scanning electron microscope in the low cycle fatigue regime at strain amplitudes in the range of $1.1 - 3.2 \cdot 10^{-3}$. It was found that HPT processed ultra-fine grained copper is prone to cyclic softening, which is a consequence of grain coarsening in the absence of shear banding in the micro samples. Novel insights into the grain coarsening mechanism were revealed by quasi *in-situ* EBSD scans, showing i) continuous migration of high angle grain boundaries, ii) preferential growth of larger grains at the expense of adjacent smaller ones, iii) a reduction of misorientation gradients within larger grains if the grain structure in the neighborhood is altered and iv) no evidence that a favorable crystallographic orientation drives grain growth during homogeneous coarsening at moderate accumulated strains, tested here.

© 2016 Acta Materialia Inc. Published by Elsevier Ltd. This is an open access article under the CC BY-NC-ND license (<http://creativecommons.org/licenses/by-nc-nd/4.0/>).

1. Introduction

Grain size reduction by severe plastic deformation (SPD) is well established to synthesize bulk ultrafine-grained (UFG) or nanocrystalline (NC) samples. Similar to the static strength, the performance in the high cycle fatigue (HCF) regime has been proven to be enhanced significantly compared to the coarse grained (CG) counterparts for UFG [1–4] and NC materials [5–8]. The reason for enhanced fatigue limits or HCF performance can be explained by a shift of the onset of microplasticity, necessary to induce fatigue damage, to higher stress levels than in the CG condition. Unfortunately, the performance of such materials in the low cycle fatigue (LCF) regime, where higher plastic strain amplitudes are present, is deteriorated and cyclic softening is promoted. For UFG materials, which will be in the focus of the current work, cyclic softening has been found to occur not only under strain controlled conditions (decreasing stress amplitude) for purity levels above 99.9% [9–12], but also in stress controlled experiments above a certain stress amplitude, where the softening is reflected in a continuously

increasing strain amplitude [11,12]. However, these studies have conflicting viewpoints about the impact of the strain amplitude. Although it is frequently reported that cyclic softening is more pronounced at higher strain amplitudes [1,13,14], other experiments show that low strain amplitudes and the concomitant enhanced lifetime enable time dependent thermally activated processes to occur and promote cyclic softening [11]. Also, material parameters can be decisive for the occurrence or magnitude of cyclic softening, for instance, a high purity level [14] or the grain shape [1]. Although it is well known that different SPD procedures generate materials of different grain boundary structures, the grain boundary misorientation has been disregarded in the context of the cyclic mechanical response for a long time. Although cyclic softening was revealed for structures consisting of major fractions of low angle grain boundaries (LAGB) [1] or high angle grain boundaries (HAGB) [11], their direct influence has not been investigated systematically.

For UFG materials, three mechanisms have been found to contribute to the observed cyclic softening, which are i) shear band formation, ii) coarsening of the fine scaled grain structure [15,16] as well as iii) a reduction of the defect density, in especially dislocation density [3,9], or a combination of them. These mechanisms can lead

* Corresponding author.

E-mail address: marlene.kapp@stud.unileoben.ac.at (M.W. Kapp).

to early strain localization, fatigue damage and failure of the samples. The small grain size and the resulting large grain boundary fraction was suspected to be responsible for these microstructural instabilities as it offers large driving forces for grain growth.

Despite the extensive work carried out on this topic, detailed knowledge about the initiation and evolution of these structural instabilities is still at its infancy. As an example, the nature of the grain growth process in these fine-scaled structures is currently not completely understood. A thorough description, whether grain growth proceeds in discrete events or in a rather continuous manner, if a certain incubation time is needed, or which grains will start to grow, is still unclear. Further issues include whether a certain crystallographic orientation is favored to grow or shrink, as well as the importance of the grain boundary type (LAGB, HAGB).

The ambiguities about the processes inducing structural instabilities prevent an understanding of how cyclically stable materials need to be designed. A sound identification of the driving forces for the underlying processes and how they evolve are of utmost importance to control the microstructural stability in a successful way.

To gain a thorough understanding about the mechanisms occurring during cyclic loading of UFG structures, a suitable experimental setup was looked for. Cyclic micro bending experiments, conducted inside a scanning electron microscope (SEM), allow for a unique correlation between changes in the microstructure and the local stress-strain state. Further, tracing the same sample area throughout the entire experiment enables the detection of crucial changes in the surface morphology, for instance shear bands or fatigue cracks which in turn may affect the softening process. Special emphasis was placed on the identification of possible correlations between boundary misorientation and crystallographic orientations with structural instabilities.

2. Experimental

Quasi constrained high pressure torsion (HPT) [17] was used to synthesize an oxygen free high conductivity (OFHC) copper (99.95%) with ultrafine grains. The HPT disk diameter d and its thickness t were 15 mm and 7.5 mm, respectively. Deformation was conducted at a pressure of 3.5 GPa for 15 revolutions n , which resulted in an equivalent v. Mises strain ϵ_{eq} of 87 at an HPT radius r of 12 mm, from which the sample was extracted, according to Eq. (1)

$$\epsilon_{eq} = \frac{2\pi nr}{t\sqrt{3}}. \quad (1)$$

Such strains are sufficient to obtain constant mechanical and structural properties throughout the entire HPT disk, except the very center ($r < 1$ mm). In this steady state region the grain size was measured by electron back scatter diffraction (EBSD) to be 530 nm (area weighted).

For the cyclic micro bending experiments, a platelet was extracted from regions of saturated microstructure, which was subsequently cut into rods of 1 mm \times 1 mm in cross-section. The top of the rods were electrochemically etched to form tips, where the final bending beam was focused-ion-beam (FIB) milled with a Zeiss LEO 1540 XB dual beam FIB workstation. For the bending beams, thickness to length ratios between 1:1 and 1:2 were used. A schematic drawing of a bending beam is shown in Fig. 1. The actual size of all samples tested can be found in Table 1.

To illustrate the mechanical and the structural changes, two samples have been selected for this study, denoted sample A and B. The cyclic micro bending experiments were conducted inside a SEM (Zeiss LEO982) using an ASMEC UNAT (sample A) and a Hysitron PI85 (sample B) microindentation system to impose the

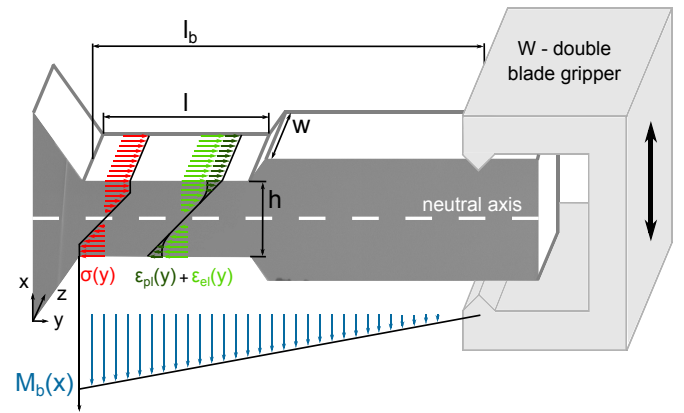


Fig. 1. Schematic drawing of a miniaturized bending beam with dimension labels of the width w , height h , length l and bending length l_b , as well as the distribution of the normalized bending moment $M_b(x)$ along the x -axis. Strain $\epsilon(y)$ and stress $\sigma(y)$ values along the y -axis are indicated.

strain amplitude. A FIB milled tungsten double blade gripper was used to impose the cyclic load onto the samples. The bending beams were loaded under displacement control, resulting in plastic strain amplitudes $\epsilon_{a,pl}$ of $1.1 - 3.2 \times 10^{-3}$ at the outer fiber, with a stress ratio $R = -1$ at a strain rate $\dot{\epsilon}$ in the range of $2.6 - 3.8 \times 10^{-3} s^{-1}$ (for details see Table 1). For sample B EBSD scans were conducted after 100, 200, 300 and 400 cycles to track the coarsening process.

The elastic contributions of the measured displacement stemming from the needle, SEM-stage and the specimen holder were taken into account by correcting the measured compliance using a method according to Wurster et al. [18]. The outer fiber stress σ_s was calculated from the force-displacement data, based on elastic bending beam theory according to Eq. (2):

$$\sigma_s = \frac{6Fl_b}{wh^2} \quad (2)$$

Although this is a good approximation for small strain amplitudes, it overestimates the stress at larger strain amplitudes. The outer fiber strain ϵ_s according to Eq. (3):

$$\epsilon_s = \frac{uh}{2ll_b} \quad (3)$$

is simply derived from the applied displacement and assumed to be constant in the gauge length. The measured force is F , the bending length l_b , gauge section width w , gauge section height h , the beam deflection u and the gauge section length l .

3. Results

3.1. Cyclic hysteresis loops

The cyclic hysteresis loops of sample A are shown in Fig. 2 for two different plastic strain amplitudes, $\epsilon_{a,pl} = 1.1 \cdot 10^{-3}$ (a) and $1.9 \cdot 10^{-3}$ (b-d), respectively. For both strain amplitudes only certain cycle numbers (90, 990, 2990, 4990, 5790 for $\epsilon_{a,pl} = 1.1 \cdot 10^{-3}$ and 90, 790, 990, 1190 after the increase to $\epsilon_{a,pl} = 1.9 \cdot 10^{-3}$) are plotted to ensure a better visibility. The maximum tensile and compressive surface stresses at the lower strain amplitude $\epsilon_{a,pl} = 1.1 \cdot 10^{-3}$ in Fig. 2a stay nearly constant up to 5790 cycles, corresponding to an accumulated plastic strain $\epsilon_{acc,pl}$ of 25.5 according to Eq. (4):

Table 1

Dimensions in μm of the tested bending beams with width w , height h , length l and bending length l_b and the testing parameters strain rate $\dot{\epsilon}$ in s^{-1} , plastic strain amplitude $\epsilon_{pl,a}$, the number of cycles N and the total applied accumulated plastic strain $\epsilon_{acc,pl}$.

	h	w	l	l_b	$\dot{\epsilon}$	$\epsilon_{a,pl}$	N	$\epsilon_{acc,pl}$
Sample A (step I)	5.0	7.5	10.0	42.0	2.6×10^{-3}	1.1×10^{-3}	5800	25.5
Sample A (step II)	5.0	7.5	10.0	42.0	3.8×10^{-3}	1.9×10^{-3}	1200	34.6
Sample B	3.4	3.3	2.7	12.6	3.1×10^{-3}	3.2×10^{-3}	400	5.1

$$\epsilon_{acc,pl} = 4 * \epsilon_{a,pl} * N \quad (4)$$

However, an increase of the applied plastic strain amplitude of sample A to $1.9 * 10^{-3}$ (Fig. 2b–d) causes a continuous drop in the maximum surface stresses during 1190 cycles, corresponding to an accumulated plastic strain of 34.6. The estimated maximum surface stress drops by 5% and 7% of the maximum stress, from 541 and -595 MPa to 515 MPa and -552 MPa, at the maximum of the positive and negative displacement deflection after 1190 cycles, respectively.

3.2. Changes in the surface morphology

In addition to the cyclic stress-strain response of the samples, SEM images were taken to capture possible changes of the surface morphology. SEM images taken from the outer fiber side surface of sample A in Fig. 3a show that cyclic bending for 5800 cycles at $\epsilon_{a,pl} = 1.1 * 10^{-3}$ ($\epsilon_{acc} = 25.5$) and for additional 1200 cycles at

$\epsilon_{a,pl} = 1.9 * 10^{-3}$ ($\epsilon_{acc} = 34.6$) already caused a significant degradation of the sample surface. A very local roughening becomes visible at the transition from sample head to the gauge section, where the maximum bending moment and thus, stresses and strains, are applied to the cantilever. Sample B (Fig. 3b) shows similar features of surface damage at the highly strained region of the cantilever consisting of severe depressions and protrusions. However, although surface roughening serves as a precursor for fatigue crack initiation, those have not been observed at the surface. Furthermore, shear or cyclic slip bands emerging at the sample surface are frequently reported for ECAP processed samples [3], but are not visible on the micro cantilever surfaces.

3.3. Changes in microstructure

As mentioned earlier, the observed cyclic softening could be a consequence of grain coarsening. To capture structural changes during cyclic loading, BSE images of the cantilever were recorded.

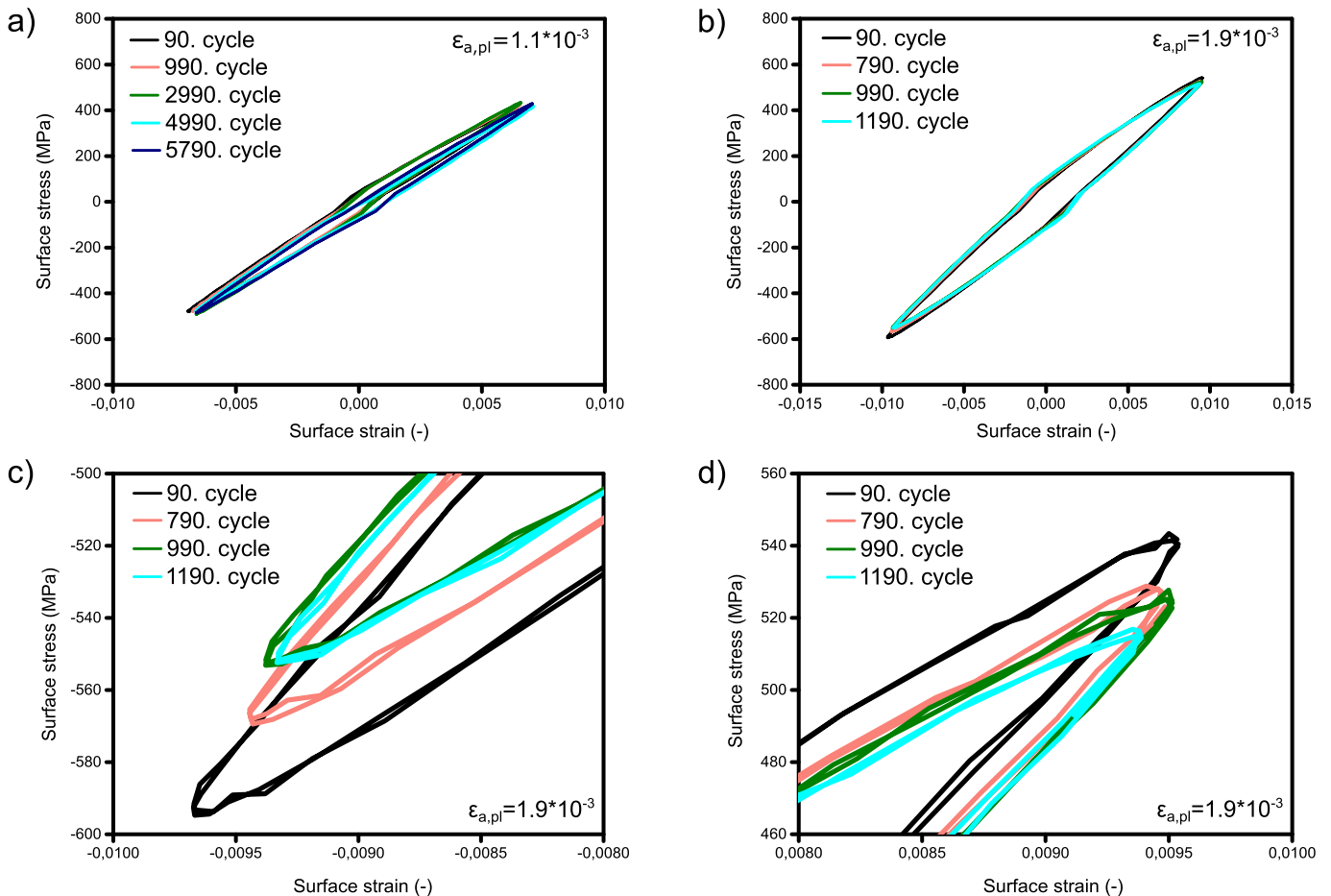


Fig. 2. Cyclic hysteresis loops for strain amplitudes of a) $\epsilon_{a,pl} = 1.1 * 10^{-3}$ and b-d) $\epsilon_{a,pl} = 1.9 * 10^{-3}$. a) No changes in the maximum surface stress were observed for the smaller strain amplitude, b) whereas cyclic softening occurred for the larger strain amplitude at the maximum of the c) negative and d) positive displacement deflection.

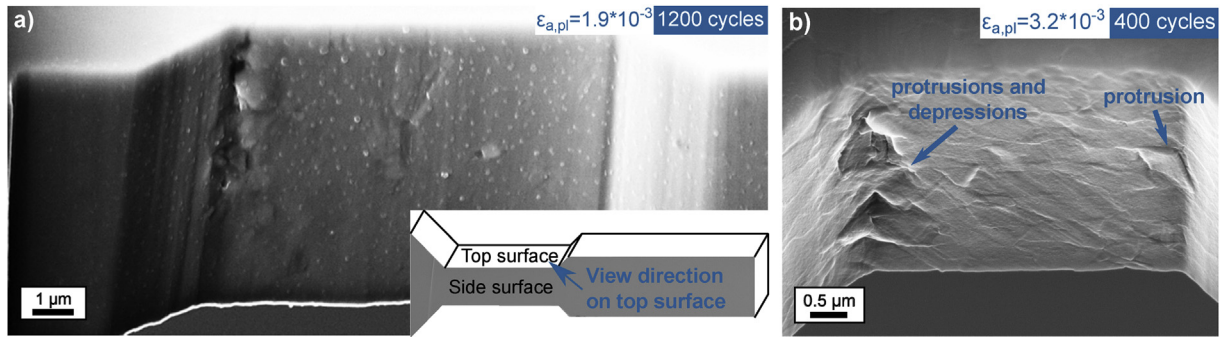


Fig. 3. Localized damage initiation at the highly strained region (outer fiber, clamping) of a) sample A tested at $\epsilon_{a,pl} = 1.9 \cdot 10^{-3}$ and b) of sample B tested at $\epsilon_{a,pl} = 3.2 \cdot 10^{-3}$ taken after 400 cycles with protrusions and depressions.

BSE images shown in Fig. 4 were taken from the side surface and from the top surface of FIB prepared cross-sections (labelled 1, 2, 3) of sample A in a certain distance from the neutral axis as marked in the schematically drawn cantilever. Considering that a plastic strain amplitude of $1.9 \cdot 10^{-3}$ is applied to a cantilever of $7.5 \mu\text{m}$ width, the maximum plastic strains occur at the outer fiber region, whereas near the neutral axis, the cantilever will still deform approximately elastically (see stress-strain distribution schematically drawn in Fig. 1). Inherent to the bending geometry, the magnitudes of the elastic strains and stresses are applied in terms of a gradient along the side surface in Fig. 4, decreasing towards the neutral axis, where they finally disappear. As a consequence, during cyclic bending the grain size evolves heterogeneously along the cantilever width. Near the neutral axis, a region with low stress-strain values, the grain size has not changed significantly (Fig. 4, side surface), compared to the initial state. This is also visible in the BSE images of the top surface (see image labelled 1), reflecting the microstructure in the thickness direction of the cantilever. In regions closer to the outer fiber, where larger strains are active, single grains have already coarsened, approaching more than $1 \mu\text{m}$ in size (see image labelled 2). This coarsening is even enhanced at the outer fiber, where the maximum stress and strain is present, resulting in single grains, which have grown up to almost $2 \mu\text{m}$ in size (see image labelled 3), still embedded in an UFG matrix, where limited grain growth occurred.

To analyze the mechanisms of grain coarsening in more detail (e.g. crystallographic orientation of growing grains), sequential EBSD scans of the gauge section were performed throughout the experiment on sample B. These results are depicted in Fig. 5. At first glance, a comparison of the IPF maps (top row) between the as-HPT processed material (0 cycles, Fig. 5a), the state after 100 cycles (Fig. 5b), 200 cycles (Fig. 5c), 300 cycles (Fig. 5d) and 400 cycles (Fig. 5e) does not yield major differences. However, a closer look manifests three different processes that occur manifoldly at various positions of the cantilever. The identified processes are: growth of larger grains, appearance of new grains and reduction of misorientation gradients. Examples at positions where these processes occurred are shown in the magnified details (labelled 1, 2, 3) in Fig. 5a–e). Firstly, a growth of larger grains at the expense of adjacent smaller grains was captured frequently (second row). For example, it can be seen that the grain boundary of the larger grain (turquoise) migrates towards the bottom left in the direction of the smaller adjacent grain (orange), which continuously shrinks until it finally disappears after 400 cycles (see Fig. 5e). Secondly, a new grain appeared and grows during cycling (see light green grain in third row). Although it cannot be proven, this process might be explained by the fact that a growing grain from just below the surface consumed grains partially covering the observed surface.

Thirdly, a reduction of misorientation gradients, seen as LAGB with small misorientation angles, appeared in certain grains (forth row). This is illustrated for a pink grain, exhibiting a misorientation of 4.2° in the undeformed state (Fig. 6a), which is removed after 100 cycles (Fig. 6c). However, misorientation gradients are not necessarily removed, as shown for a purple grain with an initial misorientation gradient of 5.1° (Fig. 6b) retaining a misorientation gradient of 4.9° after 100 cycles (Fig. 6d). It should be mentioned that these processes do not occur in an isolated way. Quite on the contrary, many structural changes of the grain structure occur as a consequence of a combination of the mentioned processes. For instance, in detail 2) a new grain appears (light green) and undergoes a growth procedure similar as remarked for detail 1) with the addition that growth occurs in every grain direction, so that it has eventually more than doubled its size. Similarly, also the reduction of misorientation gradients in detail 3) is accompanied by the migration of the grain boundary and a distinct expansion of the grain size.

4. Discussion

Cyclic softening in strain controlled fatigue experiments under LCF conditions has been frequently observed in the past for high purity copper or aluminum [1,3,9,11,12,19]. In these experiments, the principal structural changes responsible for early strain localization and thus a deteriorated mechanical performance have been identified. These changes include shear band formation, grain coarsening [11,19] and a reduction of the initial dislocation density [3]. Despite the vast number of studies, the basic mechanisms leading to structural instabilities, or how they can be avoided, could not be identified.

Most of the studies mentioned above have been conducted on UFG metals synthesized by ECAP. The reported mechanical and microstructural instabilities therein refer to microstructures of different grain shape (equiaxed, elongated) and grain boundary structures (different fraction of HAGB and LAGB), depending on the chosen ECAP route and number of passes [20]. ECAP structures synthesized by a large number of passes are especially characterized by a majority of HAGB, which is similar to HPT structures. Due to the large strains applied during HPT, the structure of the current work consists of about 80% HAGB and 20% LAGB [21]. The cyclic hysteresis loops in Fig. 2 confirm that also the HPT structure is prone to cyclic softening, akin to ECAP structures, where the cyclic stress decreases after just 20 cycles at a comparable plastic strain amplitude of $\epsilon_{a,pl} = 1 \cdot 10^{-3}$ [11]. There, the pronounced macroscopic softening stems from a severe localization of the applied cyclic strain in shear bands, where the coarsening process seems to be enhanced. In the present study, SEM images of the tested

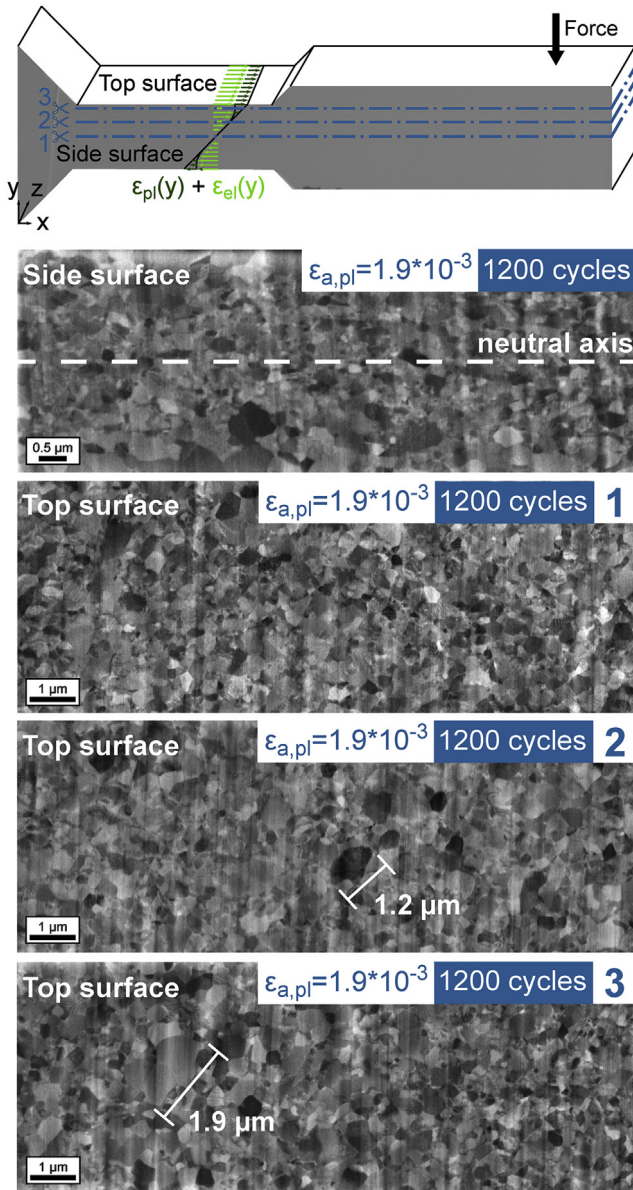


Fig. 4. BSE images of the side surface of sample A after 1200 cycles at $\epsilon_{a,pl} = 1.9 \cdot 10^{-3}$ show a gradient in the grain size evolution, which increases from the neutral axis towards the outer fiber. BSE images from the top surfaces confirm a smaller grain size in the region near the neutral axis (position 1), which increases with increasing strain amplitude (position 2) and shows grains with a size of a few micrometers near the outer fiber (position 3).

cantilevers indicate that a homogeneous grain size increase after cyclic loading (Fig. 4) is responsible for the degradation of the stress response. Although the occurrence of grain coarsening correlates to observations for ECAP structures [11], no shear bands developed during the number of cycles tested (Figs. 3 and 4). It should be mentioned that the homogeneous and moderate grain coarsening could be a consequence of the micro mechanical setup, which does not allow for large scale shear bands to form due to the confined sample dimensions. Furthermore, it is assumed that the homogeneous grain coarsening does not weaken the cyclic strength as much as in the case when severe grain growth is localized in large scale shear bands. Beside grain growth, a reduction of the dislocation density has been found to contribute to cyclic softening as the grain boundary becomes more defined during the fatigue

experiment [3]. This results are consistent with the seminal work of Feltner and Laird, where cold worked structures, consisting mainly of cells of LAGB type, were tested in the LCF regime [22,23]. Similarly as in the ECAP structures, the cell walls appeared sharper after the fatigue experiment and in addition also defects in the cell interior were less frequently found [23]. Although defect densities have not been measured directly in the present work, such changes in the dislocation content have been found to occur most prominent during the very first cycles, while for larger cycle numbers changes in the hysteresis loops become negligible [23,24]. These results seem plausible even for UFG structures tested here, as excess dislocations may annihilate easily at the numerous grain boundaries until a certain density, sufficient to realize a given plastic strain amplitude is reached. However, the results of this micro bending experiment show continuous softening up to accumulated strains of 34.6. For this reason, although contributions to the softening from a reduction in the dislocation density cannot be excluded for the very first cycles, in the authors' opinion the main reason for the cyclic softening observed here, is a consequence of grain coarsening.

An often and controversially discussed parameter influencing the amount of cyclic softening is the applied strain amplitude. Whereas many studies report enhanced cyclic softening for larger strain amplitudes [1,14,25], other works show more pronounced softening for low strain amplitudes, where the extension of the lifetime should promote thermally activated grain growth. In that context, the accumulated plastic strain $\epsilon_{acc,pl} = 4N\epsilon_{a,pl}$, which additionally takes into account the number of cycles tested, is an often overlooked parameter. For instance in the work of Höppel and Mughrabi [11] the increased cycles to failure observed at a lower strain amplitude ($N_f = 160014$ and $\epsilon_{a,pl} = 2 \cdot 10^{-4}$) lead to a larger accumulated plastic strain as compared to a higher plastic strain amplitude ($\epsilon_{a,pl} = 1 \cdot 10^{-3}$ and $N_f = 6552$). Consequently, the

enhanced cyclic softening ratio $CSR = 1 - \frac{\Delta\sigma}{\frac{\Delta\sigma}{2} \frac{N_f}{2}}$, taking into account the stress drop at half of the sample lifetime $\frac{\Delta\sigma}{2} \frac{N_f}{2}$, revealed for the lower plastic strain amplitude accords to a higher accumulated plastic strain. Solely considering the plastic strain amplitude in the current results would suggest that a minimum plastic strain amplitude is required for the onset of cyclic softening, which was absent until the plastic strain amplitude was increased to $1.9 \cdot 10^{-3}$. It is important to note, that cyclic softening did not only go along with an increased plastic strain amplitude, but also with an increased accumulated plastic strain due to an increased cycle number. Although the simultaneous linear increase of strain amplitude and accumulated strain of the experimental procedure does not allow to unambiguously differentiate, which parameter is responsible for the onset of cyclic softening, the accordance with the work of Höppel and Mughrabi [11] suggests that the accumulated strain is decisive for the onset of softening mechanisms and the subsequent degradation of the cyclic stress.

For the comparison of the micro bending experiment with macro experiments it is important to take into account that i) micro bending samples have a strong strain gradient and hence, a gradient in strain amplitude and accumulated strain, ii) in macro samples the coarsening is related to the macroscopic strain amplitude and the accumulated macroscopic strain, however, coarsening occurs often in shear bands, iii) no shear bands are formed in micro samples, therefore homogeneous coarsening takes place, which is more pronounced at the outer fiber due to the mentioned gradient. Although the stress amplitude also obeys a gradient, the stresses applied to the outer fiber region are nearly constant as soon as the yield stress is reached. Assuming for simplicity a linear cyclic stress increase from the neutral axis to the

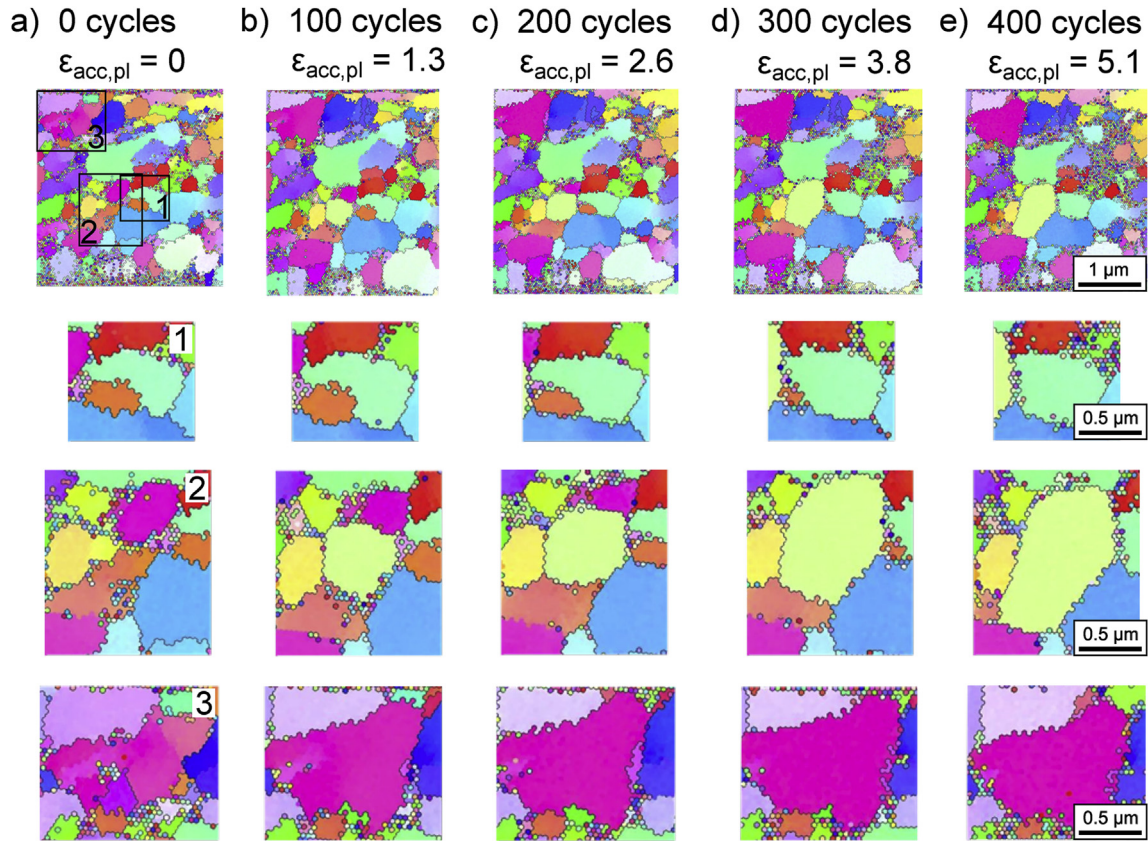


Fig. 5. EBSD images of a) the initial structure and after b) 100, c) 200, d) 300 and e) 400 cycles show that in most cases large grains grow at the expense of smaller grains (example shown for position 1), a suddenly appearing grain continuously grows (example shown for position 2) and misorientation gradients disappear in large grains (example shown for position 3).

outer fiber, one can calculate at which cantilever height the applied stress equals the yield stress, which has been found to be around 443 MPa UFG copper of 99.97% purity [26]. For the lower applied plastic strain amplitude of $1.1 \cdot 10^{-3}$ the macroscopic yield stress barely catches the outer fiber region, whereas at the larger plastic strain amplitude of $1.9 \cdot 10^{-3}$ the yield stress is reached at a distance of 500 nm from the outer fiber. Interestingly, grain growth occurs even in a larger distance of $1.5 \mu\text{m}$ away from the outer fiber (Fig. 4, side surface view), where the cyclic stress is with 340 MPa, distinctly lower than the macro yield stress. However, micro yielding will take place.

As mentioned earlier, shear banding does not contribute to the observed softening, at least at these low accumulated plastic strains. Thus, the significant contribution to the observed softening must necessarily arise from grain coarsening. The main questions of the coarsening process are still unresolved, for instance: i) Is the nature of the grain growth process of continuous or discontinuous manner and does it occur immediately or is a certain incubation time needed? ii) Is the type of grain boundary relevant for grain coarsening? iii) Do crystallographic orientations exist, which preferentially grow? iv) Is the driving force for grain coarsening of thermal or mechanical nature? v) What is the direct impact on the mechanical response? The clarification of these ambiguities is of utmost importance and will be stressed with regard to the present results in the following paragraphs.

i) It was argued in the past that grain coarsening in cyclically loaded OFHC UFG copper is similar to dynamic recrystallization [2,11]. However, in these experiments only the final structure could be analyzed, without any knowledge of what

happened during the cyclic loading in the structure. From the quasi *in-situ* experiments it could be deduced that grain coarsening is most likely caused by a continuous migration of grain boundaries (Fig. 5). Although the structure was not continuously traced during cyclic bending, but only after 100 cycles for the first time, it is very unlikely that a certain critical strain has to be applied to initiate the boundary migration process, as observed in classical dynamic recrystallization studies [27]. The structures tested here were already deformed to severe strains, where continuous boundary migration was found to occur, restoring an equilibrium structure which consists only of deformation texture components at low homologous temperatures [28,29]. Large grains were frequently observed to grow at the expense of smaller ones. This growth process seems to occur in a continuous manner, where the grain boundary migrates towards the smaller grain and continuously sweeps over it. Grain growth processes studied by *in-situ* TEM on UFG Al thin films under continuous loading conditions during nanoindentation [30] or tensile straining [31] similarly show a rapid movement of a general grain boundary whereby larger grains usually grew at the expense of adjacent smaller grains. The accordance in these two essential points with the present experiments suggests that the principal mechanisms for grain coarsening have to be the same for monotonic and cyclic loading conditions.

ii) Approximately 80% of the boundaries generated during HPT are HAGB and 20% LAGB, which are mainly observed within larger grains. The current experiments show that they react differently to the applied cyclic strain. This is in contrast to

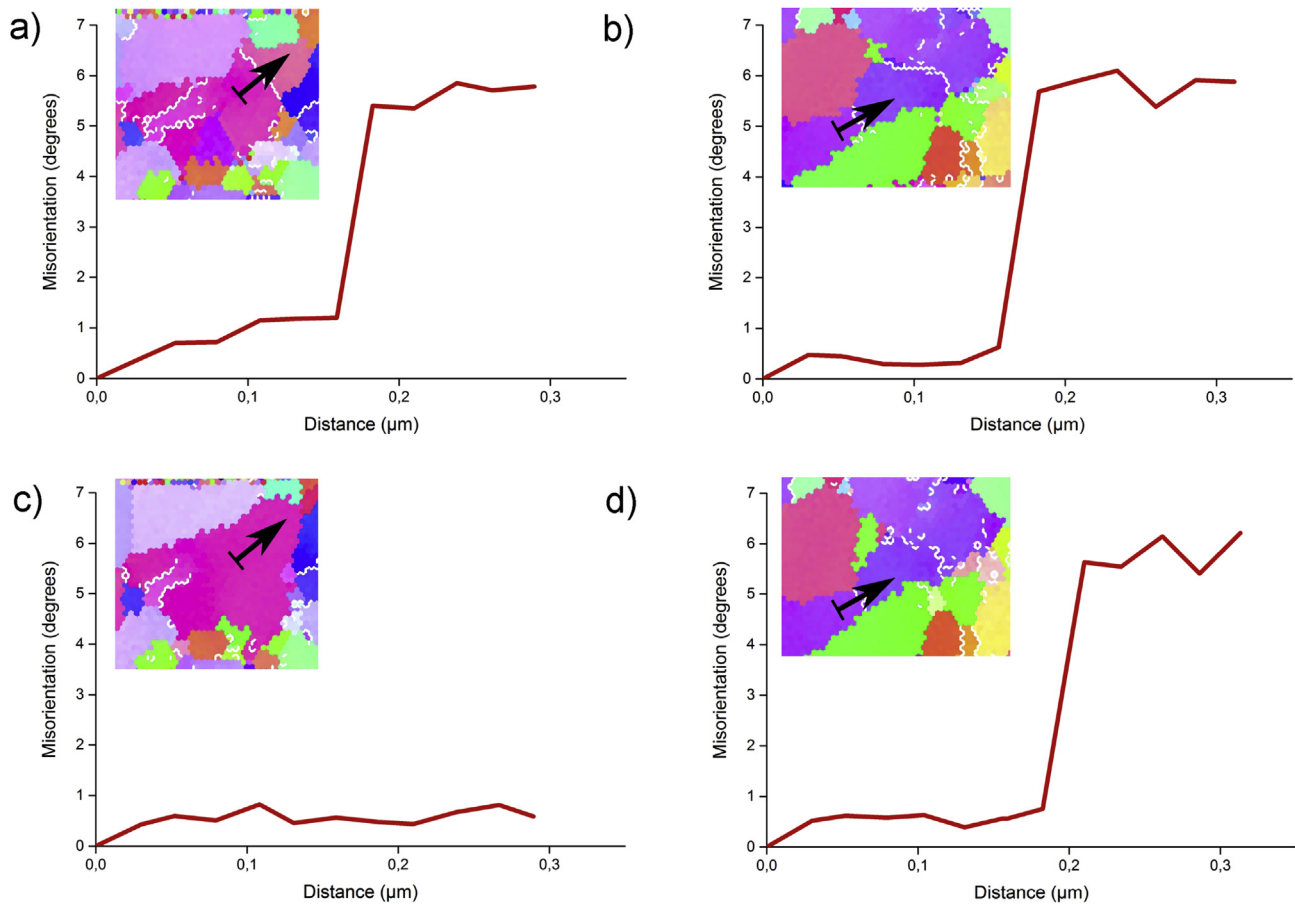


Fig. 6. a-b) Misorientation profiles within two initial grains depicted from EBSD measurements; c) misorientation gradient disappears in certain grains after 100 cycles, d) while it remains in others after 100 cycles. Lines from where misorientation profile stems are marked in the small inserts, low angle grain boundaries are drawn in white.

early studies on ECAP structures exhibiting a large fraction of low angle grain boundaries, where the main coarsening procedure was characterized by a distinct growth of the cells having small misorientation angles [9]. The current experiments clearly show, while the HAGB were the ones that cause grain growth (see HAGB as black lines for detail 1 in Fig. 5), the LAGB within the grain interior remain pretty stable, with only minor misorientation changes (see LAGB as white lines in Fig. 6b,d). Only in cases where surrounding grains in the neighborhood disappear or a migration of the boundary is observed the misorientation of the LAGB is distinctively reduced (see for instance Fig. 6a,c where blue and orange grains at the top shrink and disappear), which allows for accommodation of plastic strains. Because considerable changes of the LAGB seem only to occur if a particular grain's surroundings are changing significantly, they are likely to be classified as geometrically necessary boundaries [27]. This means that they realize a certain misorientation gradient along the grain, necessary to accommodate plastic strain with respect to the neighborhood. If the surroundings change due to growth or shrinkage, the character of this boundary is also prone to change.

- iii) As not all of the grain boundaries within the sample cross-section migrate, it is of interest, whether grains of a certain crystallographic orientation are more susceptible to grow or shrink. In an earlier study focusing on grain boundary migration during severe monotonic cold rolling of HPT processed Cu, no preferred crystallographic orientation was found to grow [28]. Quite contrary, stress differences

between neighboring grains arising from differences in the Taylor factor or the grain size led to differences in the strain energy density, which seemed to trigger the direction of the migration process [28]. However, under cyclic loading conditions, a preferential growth of a certain crystallographic orientations could not be identified in this study, at least within these low accumulated plastic strains of 5.1, as applied here.

- iv) We have shown that grain coarsening is the consequence of migrating grain boundaries. However, the decisive and most challenging question is: what drives the boundary to move? It has been argued that fatigue induced grain coarsening is thermally driven, since lower strain rates showed an enhanced effect [2]. Although certain thermal activation can never be neglected, the observation of large growing and small shrinking grains in monotonic loading tests at elevated temperatures led to the conclusion that the curvature of the grain boundary triggers the migration direction of the grain boundary [32]. Therefore, smaller grains exhibit a stronger concavity and tendency to shrink and disappear. However, this grain size effect can also be explained in lieu of the elastic strain energy. Thereby the variance in strain energy density, which is smaller in larger grains due to a lower yield stress, but larger in smaller grains due to an increased yield stress, may act as a driving force. However, since the portions are small, it is likely that at low homologous temperatures a thermal or further mechanical activation of the grain boundary is required, for instance given by the interaction between dislocations and grain boundaries [31]. Still such

processes cannot explain the eventual movement direction of the grain boundary, which determines which grain has to disappear. In our opinion, at low homologous temperatures, the difference in yield stress as a consequence of different sizes of the adjacent grains determines the shrinking grain and so triggers the migration direction of the boundary [28].

- v) Although common agreement exists concerning the contribution of grain coarsening to cyclic softening [1,2,11], it could not be identified yet to what extent this is the case. The difficulty is to differentiate the portions contributing to cyclic softening that stem from grain coarsening, compared to those from shear banding, dislocation annihilation or already formed fatigue cracks. Although the current experiments reveal a major contribution to cyclic softening from the coarsening of the ultrafine-grained structure, the impact of dislocation annihilation cannot be excluded completely. Furthermore, fatigue cracks are not visible on the side surface, however, an initiation of nanocracks from the roughened cantilever top surface cannot be excluded by experimental evidence. Therefore, the softening portion solely stemming from the cyclically induced enlargement of the grain size will not be quantified and requires a different experimental approach.

5. Conclusion

Cyclic micro bending experiments were performed on UFG OFHC copper micro cantilevers in the low cycle fatigue regime. Cyclic softening was observed, which could be explained by a coarsening of the UFG structure. Contributions to softening by shear bands could not be revealed up to an accumulated plastic cyclic strain of 34.6 in these micron sized samples. The grain growth process was studied in more detail via quasi *in-situ* EBSD measurements revealing new aspects and confirming prior observations about cyclically induced grain growth mechanisms. Hence, the main conclusions that can be drawn about cyclically induced grain growth are as follows:

- i) Grain growth increases with the accumulated plastic strain.
- ii) No preferred crystallographic orientation was observed to grow or shrink, while there seems to be a tendency for larger grains to grow at the expense of smaller grains.
- iii) Grain growth and shrinkage is realized by a continuous migration of large angle grain boundaries.
- iv) Small angle grain boundaries within larger grains seem to be geometrically necessary, as they disappear only if their neighborhood is altered.
- v) As grain growth is occurring at low homologous temperatures in regions of high plastic strain, boundary migration seems to require a mechanical activation and not, as often assumed, only large applied stresses.
- vi) As small grains tended to disappear more frequently, the migration direction seems to be triggered by differences in the elastic strain energy.

Acknowledgements

The authors would like to thank Dr. Oliver Renk for valuable discussions. Financial support by the FWF Austrian Science Fund within project number P24429-N20 is gratefully acknowledged.

References

- [1] S.R. Agnew, A.Y. Vinogradov, S. Hashimoto, J.R. Weertman, Overview of fatigue

- performance of Cu processed by severe plastic deformation, *J. Electron. Mater.* 28 (1999) 1038–1044.
- [2] H. Mughrabi, H.W. Höppel, M. Kautz, Fatigue and microstructure of ultrafine-grained metals produced by severe plastic deformation, *Scr. Mater.* 51 (2004) 807–812.
- [3] L. Kunz, P. Lukáš, M. Svoboda, Fatigue strength, microstructural stability and strain localization in ultrafine-grained copper, *Mater. Sci. Eng. A* 424 (2006) 97–104.
- [4] P. Lukáš, L. Kunz, M. Svoboda, Effect of low temperature on fatigue life and cyclic stress-strain response of ultrafine-grained copper, *Metall. Mater. Trans. A* 38 (2007) 1910–1915.
- [5] T. Hanlon, Grain size effects on the fatigue response of nanocrystalline metals, *Scr. Mater.* 49 (2003) 675–680.
- [6] T. Hanlon, E. Tabachnicova, S. Suresh, Fatigue behavior of nanocrystalline metals and alloys, *Int. J. Fatigue* 27 (2005) 1147–1158.
- [7] B.L. Boyce, H.A. Padilla, Anomalous fatigue behavior and fatigue-induced grain growth in nanocrystalline nickel alloys, *Metall. Mater. Trans. A* 42 (2011) 1793–1804.
- [8] O. Renk, A. Hohenwarther, R. Pippan, Cyclic deformation behavior of a 316L austenitic stainless steel processed by high pressure torsion, *Adv. Eng. Mater.* 14 (2012) 948–954.
- [9] S. Agnew, J. Weertman, Cyclic softening of ultrafine grain copper, *Mater. Sci. Eng. A* 244 (1998) 145–153.
- [10] S. Hashimoto, Y. Kaneko, K. Kitagawa, A. Vinogradov, R.Z. Valiev, On the cyclic behavior of ultra-fine grained copper produced by equi-channel angular pressing, *JMN* 2–6 (1999) 593–598.
- [11] H.W. Höppel, Z.M. Zhou, H. Mughrabi, R.Z. Valiev, Microstructural study of the parameters governing coarsening and cyclic softening in fatigued ultrafine-grained copper, *Philos. Mag.* 82 (2002) 1781–1794.
- [12] L. Kunz, P. Lukáš, L. Pantelejev, O. Man, Stability of ultrafine-grained structure of copper under fatigue loading, *Procedia Eng.* 10 (2011) 201–206.
- [13] M. Wong, W. Kao, J. Lui, C. Chang, P. Kao, Cyclic deformation of ultrafine-grained aluminum, *Acta Mater.* 55 (2007) 715–725.
- [14] D. Canadina, T. Niendorf, H.J. Maier, A comprehensive evaluation of parameters governing the cyclic stability of ultrafine-grained FCC alloys, *Mater. Sci. Eng. A* 528 (2011) 6345–6355.
- [15] H.W. Höppel, Mechanical properties of ultrafine grained metals under cyclic and monotonic loads: an Overview, *Mater. Sci. Forum* 503–504 (2006) 259–266.
- [16] H. Mughrabi, H.W. Höppel, Cyclic deformation and fatigue properties of very fine-grained metals and alloys, *Int. J. Fatigue* 32 (2010) 1413–1427.
- [17] T. Hebesberger, H.P. Stüwe, A. Vorhauer, F. Wetscher, R. Pippan, Structure of Cu deformed by high pressure torsion, *Acta Mater.* 53 (2005) 393–402.
- [18] S. Würster, C. Motz, R. Pippan, Characterization of the fracture toughness of micro-sized tungsten single crystal notched specimens, *Philos. Mag.* 92 (2012) 1803–1825.
- [19] S.D. Wu, Z.G. Wang, C.B. Jiang, G.Y. Li, Scanning electron microscopy-electron channeling contrast investigation of recrystallization during cyclic deformation of ultrafine grained copper processed by equal channel angular pressing, *Philos. Mag. Lett.* 82 (2002) 559–565.
- [20] A. Mishra, B. Kad, F. Gregori, M. Meyers, Microstructural evolution in copper subjected to severe plastic deformation: experiments and analysis, *Acta Mater.* 55 (2007) 13–28.
- [21] A. Vorhauer, S. Scheriau, R. Pippan, In-situ annealing of severe plastic-deformed OFHC copper, *Metall. Mater. Trans. A* 39 (2008) 908–918.
- [22] C.E. Feltner, C. Laird, Cyclic stress-strain response of F.C.C. metals and alloys - I phenomenological experiments, *Acta Metal. Mater.* 15 (1967) 1621–1632.
- [23] C.E. Feltner, C. Laird, Cyclic stress-strain response of F.C.C. metals and alloys - II dislocation structures and mechanisms, *Acta Metal. Mater.* 15 (1967) 1633–1653.
- [24] J. Schrank, W. Prantl, H.P. Stüwe, The influence of crystal orientation on the fatigue softening behavior of severely predeformed copper, *Mater. Sci. Eng. A* 110 (1989) 61–68.
- [25] E. Thiele, R. Klemm, L. Hollang, C. Holste, N. Schell, H. Natter, R. Hempelmann, An approach to cyclic plasticity and deformation-induced structure changes of electrodeposited nickel, *Mater. Sci. Eng. A* 390 (2005) 42–51.
- [26] A. Hohenwarther, R. Pippan, A comprehensive study on the damage tolerance of ultrafine-grained copper, *Mater. Sci. Eng. A* 540 (2012) 89–96.
- [27] F.J. Humphreys, M. Hatherly, *Recrystallization and Related Annealing Phenomena*, second ed., Elsevier, Amsterdam, Boston, 2004.
- [28] O. Renk, A. Hohenwarther, S. Würster, R. Pippan, Direct evidence for grain boundary motion as the dominant restoration mechanism in the steady-state regime of extremely cold-rolled copper, *Acta Mater.* 77 (2014) 401–410.
- [29] P. Ghosh, O. Renk, R. Pippan, submitted manuscript.
- [30] M. Jin, A.M. Minor, E.A. Stach, J.W. Morris, Direct observation of deformation-induced grain growth during the nanoindentation of ultrafine-grained Al at room temperature, *Acta Mater.* 52 (2004) 5381–5387.
- [31] F. Mompou, M. Legros, A. Boé, M. Coulombier, J. Raskin, T. Pardo, Inter- and intragranular plasticity mechanisms in ultrafine-grained Al thin films: an in situ TEM study, *Acta Mater.* 61 (2013) 205–216.
- [32] F. Mompou, D. Caillard, M. Legros, Grain boundary shear-migration coupling—I. In situ TEM straining experiments in Al polycrystals, *Acta Mater.* 57 (2009) 2198–2209.